



Olive mill wastewaters extract as sustainable mild steel corrosion inhibitor in 1.0 M HCl

F. Ebich¹, R. Ramdan², M. Saadouni³, Y. El Aoufir^{4,5*}, A. Chaouiki^{4,6}, S. Skal⁵,
A. Zarrouk⁷, H. Oudda⁴, A. Essamri¹

¹ Laboratory of Agroresources and Process Engineering, University Ibn Tofail, Faculty of Sciences, Kénitra, Morocco

² Laboratory of genetics and biometrics, Faculty of Science, Ibn Tofail University,
14000 Kenitra, Morocco

³ Laboratory of Organic, Organometallic and Theoretical Chemistry, Faculty of Science, Ibn Tofail University,
14000 Kenitra, Morocco

⁴ Laboratory separation processes, Faculty of Science, Ibn Tofail University PO Box 242, Kenitra, Morocco.

⁵ Materials, Nanotechnology and Environment Laboratory, Faculty of Sciences, Mohammed V University Rabat, Morocco.

⁶ Laboratory of Environmental Engineering and Biotechnology, ENSA, University Ibn Zohr, PO Box 1136, Agadir, Morocco.

⁷ LCAE-URAC18, Faculté des Sciences, Université Mohammed 1^{er}, Oujda, Morocco

Received 01 Aug 2017,

Revised 02 Oct 2017,

Accepted 14 Oct 2017

Keywords

- ✓ Olive mill wastewaters;
- ✓ Corrosion inhibition;
- ✓ Mild steel;
- ✓ HCl
- ✓ Electrochemical methods

Y. El Aoufir : eyasminal@gmail.com

Abstract

The polyphenol extract (PPE) from olive mill wastewaters was prepared and evaluated as corrosion inhibitor for mild steel in 1.0 M HCl solution using weight loss tests, polarization and electrochemical impedance spectroscopy measurements. By fitting the gravimetric data, some kinetic parameters were estimated. The adsorption of the inhibitor on the mild steel surface obeyed Langmuir adsorption isotherm. Polarization measurements showed that the inhibitor acts as mixed inhibitor for mild steel in the acidic media. The inhibition efficiency was found to increase with a corresponding increase in the PPE concentration, and the best inhibition of 89% occurred at a PPE concentration of 4 g/L. The results of the corrosion inhibition using three different methods showed narrow differences in the obtained values between the three methods.

1. Introduction

Mild steel is a widely used alloy of iron with various industrial applications. The choice of mild steel as a preferred material for construction and other usages is attributed to its relatively low cost and high mechanical strength[1,2]. However, mild steel readily undergoes corrosion in common environments of usage. Acid solutions especially hydrochloric acid used in many industrial practices such as acid cleaning, oil-well acidizing, acid descaling etc. are typical highly aggressive media for mild steel corrosion[3,4]. The chemical compounds containing electronegative functional groups and π e⁻ systems are usually good inhibitors of corrosion for many alloys and metals in corrosive environment. These organic systems can be adsorbed on the surface of the metal through the hetero atoms such as nitrogen, oxygen and sulfur[5–9]. The structure and properties of the inhibitor molecule such as functional groups, steric factor, molecular size, molecular weight, molecular structure, aromaticity, electron density of the donor atoms and π -orbital character of donating electrons affect the adsorption of corrosion inhibitor on metal surface. There has been an increase in demand for inhibitors that are not only highly effective but are also safe for human, animals and the environment as the adverse effect of some synthetic inhibitors overrides the benefits of using it[10]. Researches into inhibitors are thus geared towards natural products, prominently extracts to obtain inoffensive inhibitors with good inhibition efficiency[11,12]. The natural derived inhibitors usually contain compounds that are heterocyclic and are made up of π bonds, N, O and S atoms[13] and these structures are believed to increase the adsorption of the inhibitors on the surface of the metals and thus decrease the corrosion rate by the means of creating a protective film on the metal. In Morocco, the olive oil industry, generates a large amount of wastes consisting of olive cake (solid waste) and vegetable waters (liquid effluents of complex composition) which must be treated to deal with pollution risks because they have great power contaminant, mainly due to high concentrations of organic matter. Their harmful effects derive largely from their polyphenol content.

In the present work, the efficiency of polyphenol extracts (PPE) from olive mill wastewaters to mitigate the corrosion of mild steel in 1 M HCl acid is examined. The effect of the concentration of inhibitor compound was investigated by electrochemical tests and weight loss tests, whereas the temperature effect was only performed at 4 g/L.

2. Experimental details

2.1. Extraction

Olive mill waste waters is delipidated by total extraction with hexane. Polyphenols are extracted from delipidated margine by ethyl acetate. The mixture is stirred and then decanted, this operation is repeated four times for the purpose of recover the maximum amount of phenolic compounds. A two-phase separation makes it possible to aspirate the supernatant composed of ethyl acetate rich in polyphenols.

2.2. Materials and test solution

The steel used in this study is a carbon steel had the following composition (atom %): 0.370 % C, 0.230 % Si, 0.680 % Mn, 0.016 % S, 0.077 % Cr, 0.011 % Ti, 0.059 % Ni, 0.009 % Co, 0.160 % Cu and the remainder iron (Fe). For electrochemical studies, 1 cm² area was exposed during each measurement. Before measurements the samples were polished using different grades of emery papers SiC (120, 600 and 1200); and then subjected to the action of a buffing machine attached with a cotton wheel and a fiber wheel having buffing soap to ensure mirror bright finish, degreased by washing with ethanol, acetone and finally washed with distilled water. The aggressive solutions of 1.0 M HCl were prepared by dilution of analytical grade 37% HCl with distilled water. The concentration range of the compound PPE used was 1 to 4 g/L.

2.3. Electrochemical tests

Electrochemical tests were carried out in a conventional three electrode cell with platinum counter electrode, saturated calomel electrode as the reference electrode and the carbon steel with the surface area of 1 cm² as the working electrode. Electrochemical experiments were conducted using impedance equipment (Tacussel Radiometer PGZ 100) and controlled with Tacussel corrosion analysis software model Voltmaster 4.

Before electrochemical tests, the working electrode was immersed in test solution at open circuit potential (OCP) for 30 min to attain a stable state. The potential of potentiodynamic polarization curves started from potential -800 mV to -200 mV vs. SCE with a scan rate of 1 mV s⁻¹. Electrochemical impedance spectroscopic studies were carried out at OCP in the frequency range of 100 kHz - 10 mHz, with 10 points per decade, at the rest potential, after 30 min of acid immersion, by applying 10 mV peak to peak voltage excitation. Nyquist plots were made from these experiments.

2.4. Gravimetric measurements

Gravimetric measurements were realized in a double walled glass cell equipped with a thermostat-cooling condenser. The mild steel specimens used have a rectangular form with dimension of 2.5×2.0×0.2 cm³ were abraded with a different grade of emery paper (320-800-1200) and then washed thoroughly with distilled water and acetone. After weighing accurately, the specimens were immersed in beakers which contained 100 ml acid solutions without and with various concentrations of PPE at temperature equal to 303 K remained by a water thermostat for 6h as immersion time. The corrosion rates (C_R) and the inhibition efficiency (η_w %) of mild steel have been evaluated from mass loss measurement using the following equations:

$$\eta_w = \frac{C_R - C'_R}{C_R} \times 100 \quad (1)$$

$$\theta = 1 - \frac{C'_R}{C_R} \Rightarrow \theta = \frac{(\eta_w \%)}{100} \quad (2)$$

Where C_R and C'_R are the corrosion rates of the mild steel in hydrochloric acid without and with the studied range of the PPE concentrations, respectively, θ is the degree of surface coverage.

3. Results and discussion

3.1. Potentiodynamic polarization curves

Potentiodynamic polarization studies were carried out to gain insights into the mechanism of the mild steel dissolution at the anode and evolution of hydrogen at the cathode in the absence and presence of different concentrations of PPE. The current-potential curves for mild steel corrosion in 1.0 M HCl without and with

different concentrations of the PPE are shown in Fig. 1. The values of efficiency $\eta_{PDP}(\%)$ are calculated using Eq. 3.

$$\eta_{PDP}(\%) = \frac{i_{corr} - i'_{corr}}{i_{corr}} \times 100 \quad (3)$$

Where i_{corr} and i'_{corr} are the corrosion current densities in uninhibited and inhibited medium, respectively.

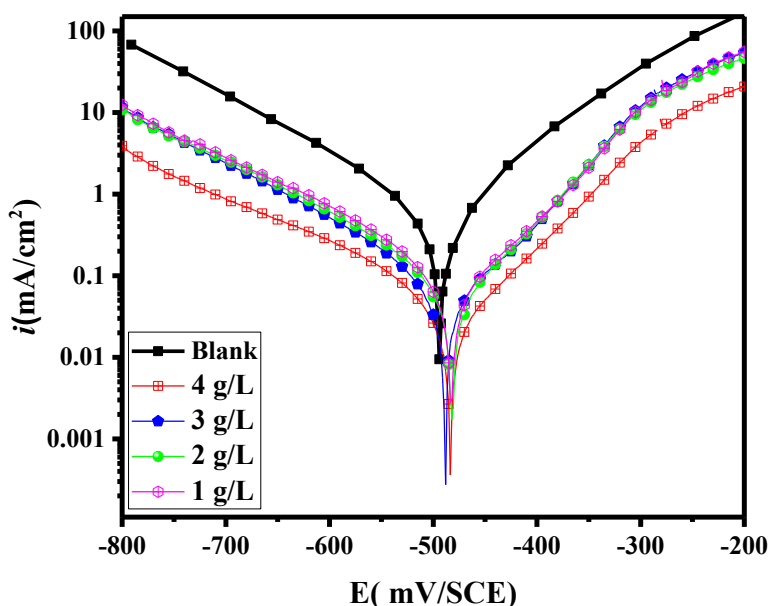


Figure 1: Polarization curves of mild steel in 1.0 M HCl for various concentrations of PPE at 303K.

Table 2: Polarization data of mild steel in 1.0 M HCl without and with various concentrations of PPE at 303 K.

Inhibitor	Concentration (g/L)	$-E_{corr}$ (mV/SCE)	$-\beta_c$ (mV/dec)	β_a (mV/dec)	i_{corr} ($\mu\text{A}/\text{cm}^2$)	η_{PDP} (%)
Blank	1M	496	162	132.2	564	-
PPE	4	485.8	159.81	104	74.3	86.82
	3	490.9	157.9	88.4	88.5	84.30
	2	484.2	155.3	90.5	105.5	81.29
	1	485.1	150.6	92.3	118.9	78.91

The polarization curves in Fig. 1 clearly reveal that the addition of the inhibitor affects both the anodic and cathodic processes as the curves are shifted towards lower corrosion current density region compared to the blank. The reduction in anodic and cathodic current densities increases as inhibitor concentration increases. This implies that the corrosion rate decreases with increasing concentration of the inhibitor and the inhibitor retard the rate of both anodic and cathodic corrosion reactions. More so, cathodic Tafel lines exhibit near parallel displacements with increasing concentration of the inhibitor, which suggests that the hydrogen gas evolution is activation-controlled and addition of inhibitor did not affect the mechanism of this process[14–16]. The similar behavior of the polarization curves both in the absence and presence of inhibitor hints that addition of the inhibitor did not alter the corrosion mechanism[17–20]. Relevant electrochemical parameters such as corrosion current density (i_{corr}) and anodic and cathodic Tafel slopes (β_c and β_a respectively) were obtained by extrapolating the linear Tafel regions of the polarization curves to the E_{corr} . The results of the electrochemical parameters together with the inhibition efficiencies are presented in Table 1. A shift in E_{corr} almost unchanged is generally attributed to mixed-type inhibitive effect of a corrosion inhibitor[21–23]. Therefore, it can be inferred that the studied PPE is mixed-type inhibitor. That is, the inhibitor retards both the anodic mild steel dissolution and the cathodic hydrogen evolution reactions. The inhibition efficiency was found to increase with concentration for the PPE studied, with the highest η_{PDP} recorded at 4 g/L.

3.2. Electrochemical Impedance Spectroscopy Measurements EIS

The effects of the inhibitor concentration on the impedance behaviour of mild steel in 1.0 M HCl solution have been studied. Nyquist plots are given in Fig. 2. It is clear from these figures that the impedance spectra obtained yields a semi-circular shape. This indicates the corrosion of the mild steel in 1.0 M HCl solution is mainly controlled by a charge transfer process[1,7,9].

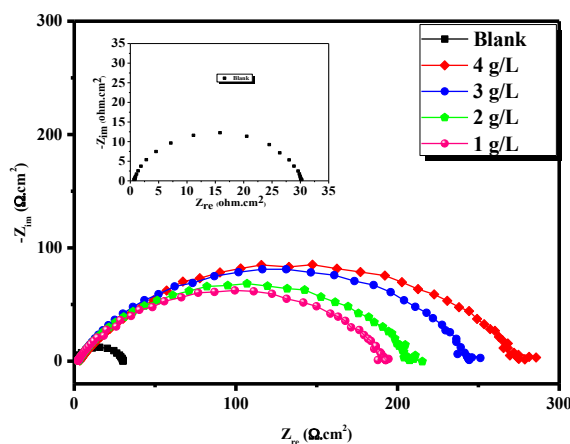


Figure 2: Nyquist diagrams for mild steel in 1.0 M HCl containing different concentrations of PPE at 303 K.

The equivalent circuit model is shown in Fig. 3 was used to analyse the *EIS* experiments, the parameters are collected in Table 2, while the double layer capacitance (C_{dl}) values are calculated using the Eq. (4)[5]:

$$C_{dl} = \sqrt[n]{Q \cdot R_{ct}^{1-n}} \quad (4)$$

where Q is the *CPE* constant and n is a coefficient that can be used as a measure of surface inhomogeneity[24]. The Eq. (5) was used to calculate the η_{EIS} (%):

$$\eta_{EIS}(\%) = \frac{R_p - R'_p}{R_p} \times 100 \quad (5)$$

Where R_p and R'_p are the polarization resistance values in with and without PPE, respectively.

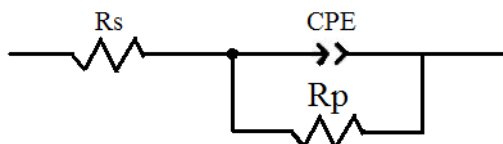


Figure 3: The electrochemical equivalent circuit used to fit the impedance spectra.

Table 2: Impedance parameters for corrosion of mild steel in 1.0 M HCl in the absence and presence of different concentrations of PPE at 303 K.

Inhibitor	Concentration (g/L)	R_{ct} ($\Omega \times \text{cm}^2$)	n	$Q \times 10^{-4}$ ($\text{s}^n / \Omega \times \text{cm}^2$)	C_{dl} ($\mu\text{F}/\text{cm}^2$)	$\eta_{R_{ct}}$ (%)
Blank	1M	29.35	0.89	1.761	91.8633	-
PPE	4	273	0.69	1.15	24.287	89.24
	3	242.3	0.75	0.997	28.488	87.88
	2	205.7	0.73	1.34	35.5013	85.73
	1	191	0.73	1.44	38.120	84.63

It is clear from Table 2 that, the corrosion of mild steel is obviously inhibited in the presence of the inhibitor. It is apparent that, the impedance response for mild steel in HCl changes significantly with increasing inhibitor concentration. It is worth noting that the similar profile of the Nyquist plots is observed in the absence and presence of the inhibitor, indicating that the addition of inhibitor do not change the mechanism for the dissolution of mild steel in HCl[4,7]. As the inhibitor concentration increased, the R_{ct} values increased, while

the C_{dl} values decrease. The decrease in C_{dl} value is due to the adsorption of inhibitor on the metal surface[7]. The inhibition efficiency increases with increasing inhibitor concentration.

3.3. Weight loss study

The weight loss results regarding the corrosion parameters for mild steel in 1.0 M HCl solution in the absence and presence of different concentrations of PPE are summarized in Table 3.

Table 3: Effect of PPE concentration on corrosion data of mild steel in 1.0 M HCl.

Inhibitor	Concentration (g/L)	C_R ($\text{mg cm}^{-2} \text{h}^{-1}$)	η (%)	θ
Blank	1M	1.135	-	-
	4	0.181	84	0.84
PPE	3	0.218	80	0.80
	2	0.289	74	0.74
	1	0.335	70	0.70

It can be seen that the inhibition efficiency increases with increase in concentration of PPE which suggests that inhibition is a result of adsorption of inhibitor on the metal surface and PPE acts as an adsorption inhibitor. The reason for the high inhibition efficiencies of this studied inhibitor towards MS may be due to the presence of several organic constituents in the extract. The results obtained from the weight loss measurements are in good agreement with those obtained from the EIS and the polarization methods.

3.4 Effect of temperature

To study the effect of temperature on the inhibition efficiency, weight loss measurements of mild steel specimens were carried out at 303, 313, 323 and 333 K with 4g/L PPE solution. The obtained corrosion rate and percentage inhibition efficiency are given in the Table 4. Inhibition efficiencies were found to decrease with increase in temperature. The decrease in inhibition efficiency with increasing temperature may be due to desorption of some adsorbed molecule from the MS surface at higher temperatures. This shows a weak adsorption interaction between MS surface and the inhibitor[25–27].

Table 4: CR and η_w % obtained from weight loss measurements of mild steel in 1.0 M HCl containing 4 g/L of PPE at different temperatures.

Inhibitors	Temperature (K)	C_R ($\text{mg cm}^{-2} \text{h}^{-1}$)	η_w (%)	θ
Blank	303	1.135	-	-
	313	2.466	-	-
	323	5.032	-	-
	333	10.029	-	-
PPE	303	0.181	84	0.84
	313	0.238	79	0.79
	323	0.329	71	0.71
	333	0.408	64	0.64

3.5. Activation parameters

The activation energy (E_a), enthalpy (ΔH^*), and entropy (ΔS^*) values shown in Table 5 were evaluated by performing PDP measurements in the temperature range of 308–338 K in the absence and presence of the optimum concentration of PPE. The activation energy (E_a), enthalpy (ΔH^*), and entropy (ΔS^*) were calculated using the following equations[1,6]:

$$i_{\text{corr}} = A \exp\left(\frac{-E_a^*}{RT}\right) \quad (6)$$

$$i_{\text{corr}} = \frac{RT}{Nh} \exp\left(\frac{\Delta H_a^*}{R}\right) \exp\left(-\frac{\Delta S_a^*}{RT}\right) \quad (7)$$

where E_a is the activation energy for corrosion of carbon steel in 1 M HCl, R is the gas constant, A is the Arrhenius pre-exponential factor, T is the absolute temperature, h is Plank's constant and N is Avogadro's number.

A plot of the corrosion current density $\ln i_{\text{corr}}$ vs. $1000/T$ resulted in straight lines, as shown in Fig. 4a. The values of E_a in 1 M HCl in the absence and presence of the inhibitor were determined from the slope. A plot of $\ln (i_{\text{corr}}/T)$ against $1000/T$, as shown in Fig. 4b, shows straight lines with a slope of $(-\Delta H^*/R)$ and an intercept of $[(\ln (R/Nh)) + (\Delta S^*/R)]$, from which the values of ΔH^* and ΔS^* were calculated.

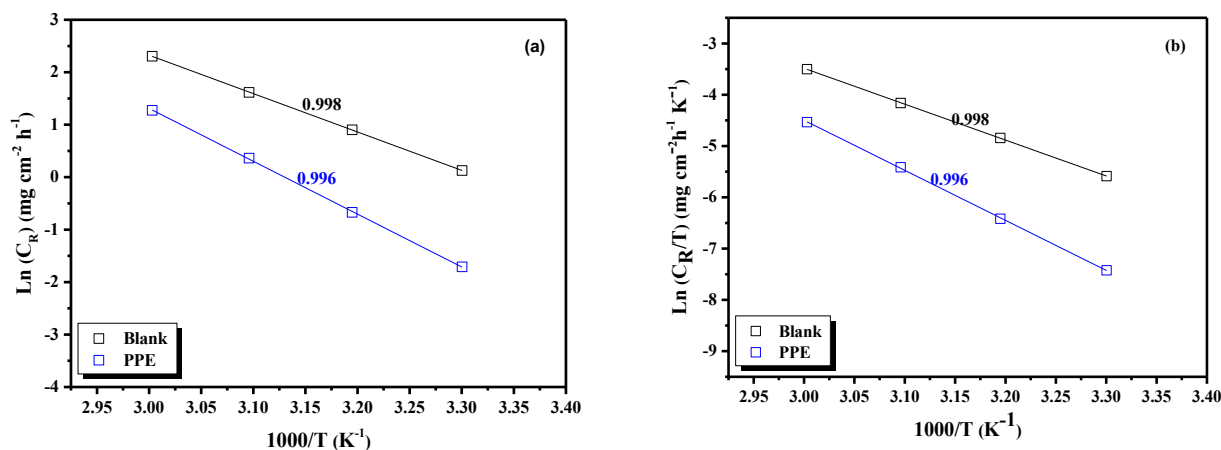


Figure 4: Arrhenius plots (a) and Transition state plots (b) for mild steel in 1.0 M HCl and 1.0 M HCl+4g/L PPE

Table 5: Corrosion kinetic parameters for mild steel in 1.0 M HCl in the absence and presence of 4 g/L PPE.

Inhibitor	E_a^* (kJ/mol)	ΔH_a^* (kJ/mol)	ΔS_a^* (J mol ⁻¹ K ⁻¹)	$E_a^* - \Delta H_a^*$
1 M HCl	26.91	24.26	-112.48	2.6
4 g/L PPE	83.72	81.06	8.48	2.6

The apparent increase in E_a and ΔH^* suggested the creation of an energy barrier to the corrosion reaction in the presence of the inhibitor. The higher value of ΔS^* for the inhibited solution might be the result of the adsorption of the PPE molecules in the 1.0 M HCl solution (quasi substitution)[28].

3.6. Adsorption isotherm

The corrosion inhibition as the process of the adsorption of inhibitor molecules on the metals surface to form a protective film has been a well-accepted explanation for the corrosion inhibition mechanism of many plant-derived inhibitors[29,30]. There are two main types of adsorption of the inhibitor molecules: physisorption and chemisorption. The adsorption of the inhibitors at a single temperature can be detailed using the adsorption isotherm models[9]. The anti-corrosion activities data were fitted into several adsorption isotherm models in order to propose the inhibition mechanism and the best fit was to the Langmuir adsorption isotherm. The Langmuir adsorption isotherm model assumes that the adsorbed molecules only occupy one site and do not interact with other molecules. It is expressed by the following formula[31]:

$$\frac{C}{\theta} = \frac{1}{K_{\text{ads}}} + C \quad (8)$$

where K_{ads} is the adsorption equilibrium constant, and C_{inh} is the inhibitor concentration. Straight lines were obtained when we plot C_{inh}/θ against C_{inh} (Fig. 5) which suggested the adsorption of inhibitor on the mild steel surface followed Langmuir adsorption isotherm. The adsorption equilibrium constant (K_{ads}) and free energy of adsorption (ΔG_{ads}) were calculated using the Equation[32]:

$$\Delta G_{\text{ads}} = -RT \ln(K_{\text{ads}} * C_{\text{solvent}}) \quad (9)$$

Where: C_{solvent} is the molar concentration of solvent (For H₂O is 999 g L⁻¹). R is universal gas constant, T is the absolute temperature.

If we assume that the major component plays the principal role in inhibition, then adsorption obeys to Langmuir isotherm. But, generally in this kind of green inhibitors (natural plants: oil or extract), inhibitory action is related to the intermolecular synergistic effect if the various components of natural oil or extract[33]. It is safely recommended to not determine $\Delta G_{\text{ads}}^\circ$ value since the mechanism of adsorption remains unknown.

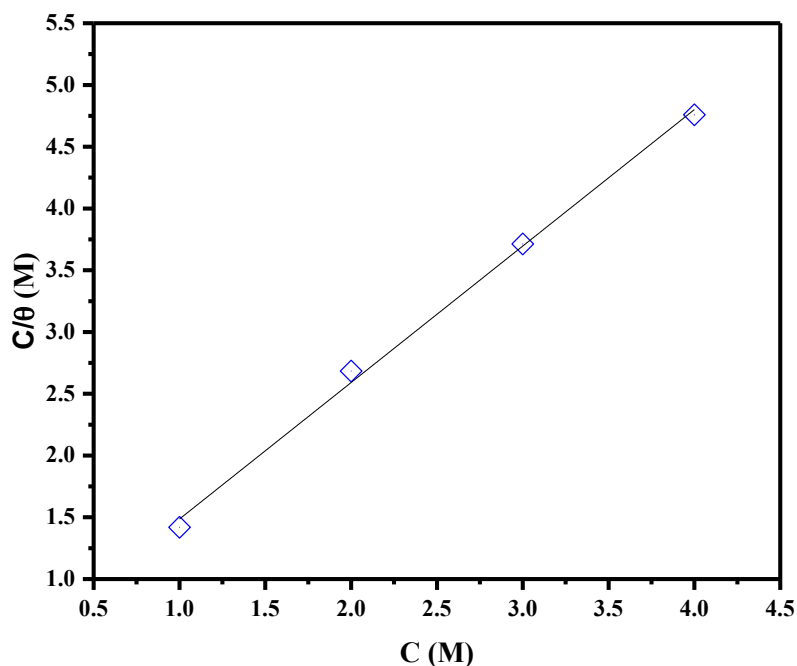


Figure 8: Langmuir adsorption of PPE on the mild steel surface in 1.0 M HCl solution at 303K.

Conclusion

The polyphenol extract (PPE) from olive mill wastewaters acts as an efficient corrosion inhibitor for mild steel in HCl acid media as evident from the weight loss and electrochemical tests. Tafel polarization studies show that PPE acts as a mixed type inhibitor. The polarization resistance (R_p) increases and the double layer capacitance (C_{dl}) decreases due to adsorption of the inhibitor molecules on the surface of mild steel. Inhibition efficiency increased with increase in additive concentration. The corrosion inhibition is achieved through the adsorption of the PPE on the mild steel surface. The adsorption process obeys Langmuir isotherm.

References:

1. R. Salghi, S. Jodeh, E.E. Ebenso, H. Lgaz, D. Ben Hmamou, I.H. Ali, M. Messali, B. Hammouti, N. Benchat, *Int. J. Electrochem. Sci.* 12 (2017) 3309–3322. doi:10.20964/2017.04.45.
2. T. Laabaissi, H. Lgaz, H. Oudda, F. Benhiba, H. Zarrok, A. Zarrouk, A. El Midaoui, B. Lakhrissi, R. Tourir, *J. Mater. Environ. Sci.* 8 (2017) 1054–1067.
3. Y. El Aoufir, J. Sebhaoui, H. Lgaz, Y. El Bakri, A. Zarrouk, F. Bentiss, A. Guenbour, E.M. Essassi, H. Oudda, *J. Mater. Environ. Sci.* 8 (2017) 2161–2173.
4. H. Lgaz, R. Salghi, S. Jodeh, B. Hammouti, *J. Mol. Liq.* 225 (2017) 271–280. doi:10.1016/j.molliq.2016.11.039.
5. M. Messali, H. Lgaz, R. Dassanayake, R. Salghi, S. Jodeh, N. Abidi, O. Hamed, *J. Mol. Struct.* 1145 (2017) 43–54.
6. R. Salghi, S. Jodeh, E.E. Ebenso, H. Lgaz, D. Ben Hmamou, M. Belkhaouda, I.H. Ali, M. Messali, B. Hammouti, S. Fattouch, *Int. J. Electrochem. Sci.* 12 (2017) 3283–3295.
7. H. Lgaz, K. Subrahmanya Bhat, R. Salghi, Shubhalaxmi, S. Jodeh, M. Algarra, B. Hammouti, I.H. Ali, A. Essamri, *J. Mol. Liq.* 238 (2017) 71–83. doi:10.1016/j.molliq.2017.04.124.
8. L. Afia, O. Hamed, M. Larouj, H. Lgaz, S. Jodeh, R. Salghi, (2017).
9. Y. El Aoufir, Y. El Bakri, H. Lgaz, A. Zarrouk, R. Salghi, I. Warad, Y. Ramli, A. Guenbour, E.M. Essassi, H. Oudda, *J. Mater. Environ. Sci.* 8 (2017) 3290–3302.
10. A.J. Bard, M. Stratmann, P.R. Unwin, 4, Wiley-VCh, 2003.
11. V. Rajeswari, D. Kesavan, M. Gopiraman, P. Viswanathamurthi, K. Poonkuzhali, T. Palvannan, *Appl. Surf. Sci.* 314 (2014) 537–545.
12. M. Shabani-Nooshabadi, F.S. Hoseiny, Y. Jafari, *Metall. Mater. Trans. A.* 46 (2015) 293–299.

13. R. Solmaz, *Corros. Sci.* 79 (2014) 169–176.
14. B. El Makrini, H. Lgaz, K. Toumiat, R. Salghi, S. Jodeh, G. Hanbali, M. Belkhaouda, M. Zougagh, *Res. J. Pharm. Biol. Chem. Sci.* 7 (2016) 2277–2285.
15. L. Adardour, H. Lgaz, R. Salghi, M. Larouj, S. Jodeh, M. Zougagh, O. Hamed, H. Oudda, *Pharm. Lett.* 8 (2016) 212–224.
16. H. Lgaz, M. Saadouni, R. Salghi, S. Jodeh, Y. Ramli, A. Souizi, H. Oudda, *Pharm. Lett.* 8 (2016) 167–179.
17. L. Adardour, H. Lgaz, R. Salghi, M. Larouj, S. Jodeh, M. Zougagh, O. Hamed, M. Taleb, *Pharm. Lett.* 8 (2016) 173–185.
18. L. Adardour, H. Lgaz, R. Salghi, M. Larouj, S. Jodeh, M. Zougagh, I. Warad, H. Oudda, *Pharm. Lett.* 8 (2016) 126–137.
19. B. El Makrini, K. Toumiat, H. Lgaz, R. Salghi, S. Jodeh, G. Hanbali, M. Belkhaouda, M. Zougagh, *Res. J. Pharm. Biol. Chem. Sci.* 7 (2016) 2286–2294.
20. K. Toumiat, Y. El Aoufir, H. Lgaz, R. Salghi, S. Jodeh, M. Zougagh, H. Oudda, *Res. J. Pharm. Biol. Chem. Sci.* 7 (2016) 1210–1218.
21. K. Toumiat, Y. El Aoufir, H. Lgaz, R. Salghi, S. Jodeh, M. Zougagh, H. Oudda, *Res. J. Pharm. Biol. Chem. Sci.* 7 (2016) 1209–1217.
22. Y. El Aoufir, H. Lgaz, K. Toumiat, R. Salghi, S. Jodeh, M. Zougagh, A. Guenbour, H. Oudda, *Res. J. Pharm. Biol. Chem. Sci.* 7 (2016) 1219–1227.
23. M. Elfaydy, H. Lgaz, R. Salghi, M. Larouj, S. Jodeh, M. Rbaa, H. Oudda, K. Toumiat, B. Lakhri, *J. Mater. Environ. Sci.* 7 (2016) 3193–3210.
24. W. Chen, S. Hong, B. Xiang, H. Luo, M. Li, N. Li, *Corros. Eng. Sci. Technol.* 48 (2013) 98–107.
25. L. Adardour, M. Larouj, H. Lgaz, M. Belkhaouda, R. Salghi, S. Jodeh, A. Salman, H. Oudda, M. Taleb, *Pharma Chem.* 8 (2016) 152–160.
26. M. Saadouni, M. Larouj, R. Salghi, H. Lgaz, S. Jodeh, M. Zougagh, A. Souizi, *Pharm. Lett.* 8 (2016) 96–107.
27. B. El Makrini, H. Lgaz, M. Larouj, R. Salghi, A. Rasem Hasan, M. Belkhaouda, S. Jodeh, M. Zougagh, H. Oudda, *Pharma Chem.* 8 (2016) 256–268.
28. D.K. Yadav, B. Maiti, M. Quraishi, *Corros. Sci.* 52 (2010) 3586–3598.
29. A. Biswas, S. Pal, G. Udayabhanu, *Appl. Surf. Sci.* 353 (2015) 173–183.
30. D. Bouknana, B. Hammouti, M. Messali, A. Aouniti, M. Sbaa, *Asian Pac. J. Trop. Dis.* 4 (2014) S963–S974.
31. H. Lgaz, R. Salghi, S. Jodeh, Y. Ramli, M. Larouj, K. Toumiat, M. Quraishi, H. Oudda, W. Jodeh, *J. Steel Struct Constr.* 2 (2016) 2472–0437.
32. H. Lgaz, O. Benali, R. Salghi, S. Jodeh, M. Larouj, O. Hamed, M. Messali, S. Samhan, M. Zougagh, H. Oudda, *Pharma Chem.* 8 (2016) 172–190.
33. H. Lgaz, O. Benali, R. Salghi, S. Jodeh, M. Larouj, O. Hamed, M. Messali, S. Samhan, M. Zougagh, H. Oudda, *Pharma Chem.* (2016) 172–190.

(2018) ; <http://www.jmaterenvirosci.com>